ACS APPLIED MATERIALS & INTERFACES

Research Article

www.acsami.org

Electric Field-Assisted Orientation of Short Phosphate Glass Fibers on Stainless Steel for Biomedical Applications

Qiang Chen,[†,‡,§] Jiajia Jing,[†] Hongfei Qi,[†] Ifty Ahmed,[∥] Haiou Yang,[‡] Xianhu Liu,[⊥] T. L. Lu,[*,†] and Aldo R. Boccaccini[*,§]

[†]Key Laboratory for Space Bioscience and Biotechnology, School of Life Sciences and [‡]State Key Laboratory of Solidification Processing, Northwestern Polytechnical University, Xi'an 710072, Shaanxi, China

[§]Institute of Biomaterials, Department of Materials Science and Engineering, University of Erlangen-Nuremberg, Cauerstrasse 6, Erlangen 91058, Germany

[∥]Faculty of Engineering, Department of Mechanical, Materials and Manufacturing Engineering, University of Nottingham, Nottingham NG 7 2RD, United Kingdom

[⊥]National Engineering Research Center for Advanced Polymer Processing Technology, Zhengzhou University, Zhengzhou 450002, China

ABSTRACT: Structural and compositional modifications of metallic implant surfaces are being actively investigated to achieve improved bone-to-implant bonding. In this study, a strategy to modify bulk metallic surfaces by electrophoretic deposition (EPD) of short phosphate glass fibers (sPGF) is presented. Random and aligned orientation of sPGF embedded in a poly(acrylic acid) matrix is achieved by vertical and horizontal EPD, respectively. The influence of EPD parameters on the degree of alignment is investigated to pave the way for the fabrication of highly aligned sPGF structures in large areas. Importantly, the oriented sPGF structure in the coating, owing to the synergistic effects of bioactive composition and fiber orientation, plays an important role in directional cell migration and enhanced proliferation. Moreover, gene expression of MC3T3-E1 cells cultured with different concentrations of sPGF is thoroughly assessed to elucidate the potential stimulating effect of sPGF on osteogenic differentiation. This study represents an innovative exploitation of EPD to develop textured surfaces by orientation of fibers in the macroscale, which shows great potential for directional functionalization of metallic implants.

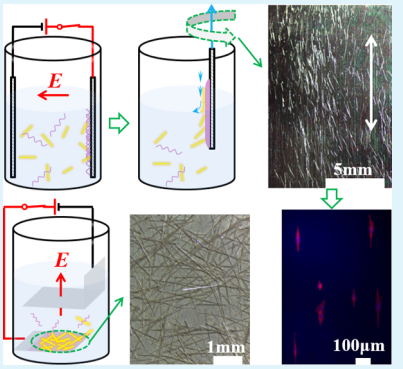

KEYWORDS: *electrophoretic deposition, phosphate glass fiber, alignment, osteogenic differentiation, bone implants*

1. INTRODUCTION

The long-term survival rate of metallic implants is usually restricted due to their bioinert character, which leads to weak bone-to-implant contact and eventually interfacial loosening in situ.[1−3] The modification of implant surfaces with biological coatings is being considered to improve osseointegration as well as to reduce risks associated with infections and corrosion.[4−6] Bioceramics, including bioactive glasses and hydroxyapatite (HA), are well-known materials to functionalize metallic implants.[7,8] Inspired by the organic/inorganic composition of natural bone, the combination of bioceramics with biopolymers to form composite coatings is gaining increasing interest.[9] Such coatings are attractive because they can be processed at room temperature and enable the incorporation of biomolecules such as antibiotics during the coating process.[10] In this way, the bioceramic acts as the bioactive filler and the biopolymer acts as a binder connecting the filler particles to the metallic substrate. Compared to hard coatings composed of pure ceramics, the presence of a compliant polymer component is expected to promote close contact between the metal implant and bone tissue.[9]

Phosphate glass fiber (PGF) possesses several attractive features in comparison to those obtained from silicate bioactive glasses,[11] e.g., PGF is completely resorbable in physiological fluids, which is in contrast to the slow/incomplete degradation of silica-based glasses. In addition, the fibrous structure of PGF enables not only the reinforcing capability in composites but also the biological functions in biomedical applications. Ahmed et al.[12] produced an iron-doped PGF, which was seen to support the attachment and differentiation of muscle precursor cells along the fiber axis. Vitale-Brovarone et al.[13] reported that PGF played an important role on neuronal polarization and further guided cell spreading. Other researches highlighted the potential of PGF in promoting the functional recovery of completely transected rat spinal cords[14] and the peripheral nerve injury[15] in the way of controlling the directional cell proliferation and differentiation. Indeed, many cell biology studies have recently highlighted the importance of structural

Received: January 24, 2018
Accepted: March 5, 2018
Published: March 5, 2018

DOI: 10.1021/acsami.8b01378
ACS Appl. Mater. Interfaces XXXX, XXX, XXX−XXX

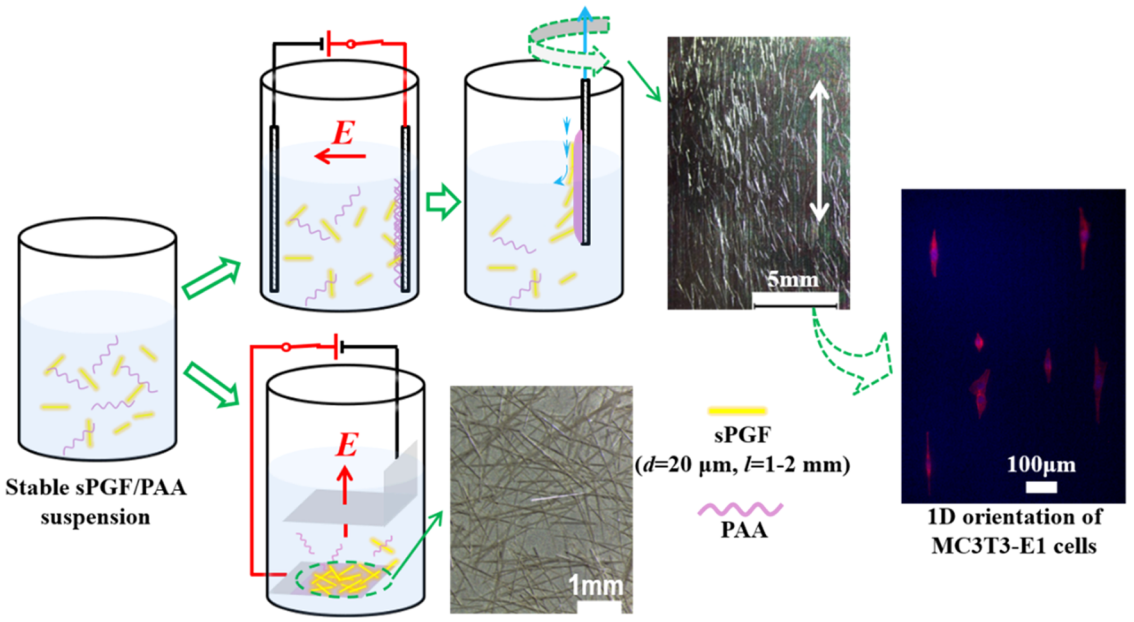

Figure 1. Vertical (top) and horizontal (bottom) EPD configurations for the production of aligned and random oriented sPGF on metallic substrates.

orientation on stimulating osteogenic behavior.[16] It is considered that random and aligned nanofibers will influence the osteogenic gene expression by affecting the cell morphology, e.g., randomly oriented fibrous scaffolds encouraged polygonal cell spreading and subsequent facilitate early osteogenic differentiation, whereas aligned fibrous scaffolds increased cell elongation and discouraged osteogenic differentiation.[17,18] However, Rowland et al.[19] found that aligned fibrous scaffolds using polydioxanone as raw material favored significantly both osteogenic and chondrogenic differentiation compared to random fibrous scaffolds. In addition, with the incorporation of bioactive components, including nanohydroxyapatite and bone growth factors, Gao et al.[20] revealed that aligned polycaprolactone nanofibers showed more osteogenic activity than randomly oriented counterparts, a result that may be assigned to a synergistic stimulation on the osteogenic differentiation through an integrin-mediated pathway. In the context of aligned fibrous coatings using PGF as building blocks, it is expected that the presence of PGF, owing to its bioactive character and fibrous geometry, will significantly promote osteoblastic activity on the surface of bone implants. Therefore, it is necessary to develop coating techniques that enable incorporation of oriented PGF in novel coating microstructures.

Indeed, numerous techniques have been developed to produce aligned patterns or fibers aiming to explore their effect on osteoblastic activity, such as electrospinning,[21,22] photolithography,[23] anodization,[24] and embossing techniques.[25] However, these techniques are mainly suitable to produce aligned patterns on free-standing membranes or on flat substrates in a relatively small size, which restricts their potential application in orthopedic implants. There is a need for straightforward, fast, and scalable patterning techniques, including methods for self-assembly of micro/nanoparticles as an alternative way to fabricate scalable patterns with controlled nanostructures.[26] In the case of short PGF (sPGF), the relative small size and high flexibility of these fibers make them promising for their assembly in aligned patterns on substrates with complex geometry and curvature. In addition, the degradation rate, mechanical properties, and biological functions can be easily changed by tailoring the ionic composition of sPGF.[27] To investigate the possible effects of sPGF on regulating the osteoblastic proliferation and differentiation, the prerequisite is to be able to manipulate the orientation of sPGF in relative large areas and in controlled manner.

Electrophoretic deposition (EPD) is a simple, rapid, and versatile coating technique that is able to control the movement of charged particles/molecules under an appropriate electric field, leading to their consolidation on the oppositely charged electrode with complex geometry and surface topography to form coatings with tailored thickness and microstructure.[28,29] According to our previous experience on EPD of oriented cellulose nanowhisker films,[30] the capability of EPD to control the orientation of sPGF in an organic−inorganic composite coating was investigated in this study. sPGF with the length of 1−2 mm were dispersed in aqueous poly(acrylic acid) (PAA) solution to obtain stable EPD suspension at first. Both aligned and random orientation of sPGF in the deposited coatings were successfully obtained with the proper design of the EPD cell and the corresponding EPD parameters, as schematically shown in Figure 1. The mineralization of the deposited coatings as well as their interaction with osteoblasts (MC3T3-E1) in vitro was investigated bearing in mind the potential application of the coatings in bone replacement devices.

2. EXPERIMENTAL SECTION

2.1. Materials. Phosphate glass fibers with the composition $40P_2O_5-24MgO-16CaO-15Na_2O-4Fe_2O_3$ in mol %—denoted as P40—were prepared as reported previously by Felfel et al.[31] Briefly, continuous fibers with a diameter of ∼15 μm were first produced via melt-draw spinning at ∼1100 °C and ∼1600 rpm, followed by annealing at the glass transition temperature (T_g = 479 °C) for 90 min. The as-prepared fiber bundles were chopped into sPGF with the length of 1−2 mm before use. Poly(acrylic acid) powder (PAA, CAS no. 9001-03-4, and molecular weight ∼ 1 250 000 kDa) and other

DOI: 10.1021/acsami.8b01378
ACS Appl. Mater. Interfaces XXXX, XXX, XXX−XXX

chemicals for simulated body fluid (SBF) preparation were purchased from Sigma-Aldrich.

2.2. EPD-Based Coating Process. PAA was first dissolved in deionized water by magnetic stirring for 10 min followed by 5 min sonication treatment using an ultrasonic bath (Bandelin Sonorex, Germany). The pH of the PAA solution was then adjusted to 8 by adding a few drops of NaOH (1 M) to induce thorough ionization of the PAA molecules.[32] sPGF were then added in the PAA solution with continuous magnetic stirring for 10 min. Different concentrations of PAA (0.5−2 g/L) and sPGF (0.25−2 g/L) were applied throughout the experiment. Before each EPD process, the blend suspension was put under continuous magnetic stirring to ensure the homogeneous dispersion of sPGF. The EPD cell included two parallel 316L stainless steel (R_a of 0.63 μm) electrodes, horizontally or vertically located, with the deposition area of 15 × 20 mm^2 and the distance of 10 mm between electrodes. It should be noted that the deposition is also feasible on other substrates with conductive surfaces. Anodic deposition is achieved via the electrophoresis of negatively charged PAA chains (due to ionization of −COOH to −COO−) followed by neutralization in the low pH region at the anode interface, as discussed in the literature.[33] According to a trial-and-error approach, processing parameters were optimized to obtain composite sPGF−PAA coatings with homogeneous and most importantly highly aligned sPGF (for vertical electrode). The deposited anode was gently withdrawn from the suspension (~2.5 mm/s) and dried horizontally in air for 30 min at room temperature, yielding the deposit mass of sPGF−PAA composite coatings in the range of 1−10 mg (or 0.33−3.3 mg/cm^2). The alignment of sPGF in the coating and their robust adhesion to the substrate were maintained due to the presence of a PAA binder layer. The concentration of PAA and sPGF in the suspension, as well as the corresponding EPD parameters intended to fabricate aligned sPGF by horizontal electric field are listed in Table 1. The alignment of sPGF in the deposited sPGF−PAA coatings was characterized by optical microscope (Leica, IC80HD).

Table 1. List of Suspensions and Corresponding EPD Parameters Using Horizontal Electric Field

sample code	PAA concentration (g/L)	sPGF concentration (g/L)	deposition voltage (V)	deposition time (s)
I	0.25	0.125	10	60
II	0.25	0.125	50	10
III	1	0.5	10	60
IV	1	0.5	20	30
V	1	0.5	30	15
VI	1	0.5	50	5
VII	2	0.5	20	15
VIII	2	1	20	15

2.3. In vitro Mineralization Study. The as-prepared coatings (e.g., sample I) were soaked in 20 mL of SBF prepared according to the literature[34] and placed in an orbital shaker at 37 °C at an agitation rate of 90 rpm. The samples were incubated for predetermined time periods and the SBF was refreshed every 2 days. Then, the samples were removed, gently rinsed with deionized water for three times and dried at 37 °C. Scanning electron microscopy (SEM) (model Auriga, Zeiss) combined with energy-dispersive spectroscopy (X-MaxN Oxford Instruments, U.K.) were applied to analyze the morphology (surface and cross section) and elemental composition of the samples after mineralization. Ion release profiles of sPGF in SBF were studied by means of inductively coupled plasma emission spectrometer (ICPE9000, Shimadzu, Japan). sPGF (0.1 g) was soaked in 50 mL of SBF and placed in an orbital shaker at 37 °C with an agitation rate of 90 rpm. After 2 h, 8 h, 1, 6, 14, and 28 days, 1 mL of the solution was extracted and filtered using 0.22 μm filter to remove possible fiber solids from the solution. The absorption wavelengths for the detection of P and Ca were selected according to the literature.[35] The calibration curves were obtained by preparing standard solutions containing P and Ca (supplied by Spex-CertiPrep, U.K.). Three replicates were measured for each element at each time point.

2.4. Cellular Studies. *2.4.1. Cell Proliferation.* MC3T3-E1 (pre-osteoblast) cells were cultured in a growth medium of Alpha minimum essential medium (Invitrogen) with 10% fetal bovine serum, 100 unit/mL penicillin, and 100 mg/mL streptomycin. Cells were incubated at 37 °C under a moist atmosphere of 5% CO_2 in air and the culture medium was refreshed every 2 days. The cell proliferation was determined using cell counting kit-8 assay (CCK-8; Dojindo, Japan). The samples were sterilized by immersion in 70 vol % ethanol for 20 min, followed by thorough rinsing with sterile phosphate-buffered saline (PBS) before use. Pure PAA coatings produced from sPGF-free suspension were chosen as the control to the sPGF−PAA coatings (sample VI in this study). 5 × 10^4 cells in 100 μL medium were first seeded on the sterilized samples (1 × 1 cm^2) located in a 24-well plate. After 4 h of incubation to ensure complete adherence of the cells on the sample, each well was supplemented with 900 μL medium. In this way, all the cells were seeded only on the sample rather than on the uncovered well plate. After culturing for 2, 4, and 7 days, 20 μL per well of CCK-8 reagent was added and the cells were incubated for additional 2 h. The results were expressed as the mean absorbance (optical density at 450 nm) of six parallel tests.

2.4.2. Cell Morphology. For cell morphology observations, the cells were incubated on both the control and the sPGF−PAA samples for 2 days following the above-mentioned protocol. The cytoskeleton of MC3T3-E1 was analyzed using filamentous actin (F-actin) staining. Briefly, the cells were fixed with 4% paraformaldehyde for 10−30 min, permeabilized with 0.1% Triton X-100 for 5 min, and blocked with 1% bovine serum albumin for 20 min. The treated skeleton and nuclei were then stained with rhodamine phalloidin (100 nM, Solarbio, China) for 20 min and Hoechst 33258 (10 μg/mL, Solarbio, China) for 5 min in the dark, respectively. The stained cells were rinsed thoroughly with PBS and then viewed under fluorescence microscopy (Nikon 80i, Japan). High-magnification images of cell morphology on the sPGF−PAA coating were obtained by SEM (model Auriga, Zeiss). The samples were rinsed with PBS and fixed with 2.5% glutaraldehyde for 3 h at 4 °C, and subsequently dehydrated in ethanol solutions of varying concentrations (30, 50, 70, 90, and 100%) for 15 min, respectively. The samples were dried in a desiccator at 37 °C and then sputter-coated with gold before SEM observation.

2.4.3. Osteogenic Differentiation Effect of sPGF. The osteogenic markers, including cell morphology, and bone-related gene expression were characterized by culturing MC3T3-E1 cells with different concentrations of sPGF (0, 1, 5 mg/mL). The expression of genes associated with osteogenesis, including runt-related transcription factor 2 (RUNX2), collagen type I (COL1α), and osteocalcin (OCN), was assessed by quantitative real-time polymerase chain reaction (qRT-PCR). Briefly, 2.5 × 10^5 cells per well were seeded in six-well plate with sPGF and cultured for 7 and 14 days. During culture, the morphology of the cells was observed by optical microscope (CKX41,

Table 2. Primer Sequences of Genes for the Quantitative RT-PCR[36]

gene name (genebank no.)	forward primer sequence (5′−3′)	reverse primer sequence (5′−3′)
RUNX2 (NM_001145920.1)	TGCACCTACCAGCCTCACCATAC	GACAGCGACTTCATTCGACTTCC
COLIα (NM_007742.3)	GAAGGCAACAGTCGATTCACC	GACTGTCTTGCCCCAAGTTCC
OCN (NM_007541.2)	AGGACCATCTTTCTGCTCACT	GCGTTTGTAGGCGGTCTTCA
GAPDH (NM_008084.2)	TGCACCACCAACTGCTTAG	GGATGCAGGGATGATGTTC

DOI: 10.1021/acsami.8b01378
ACS Appl. Mater. Interfaces XXXX, XXX, XXX−XXX

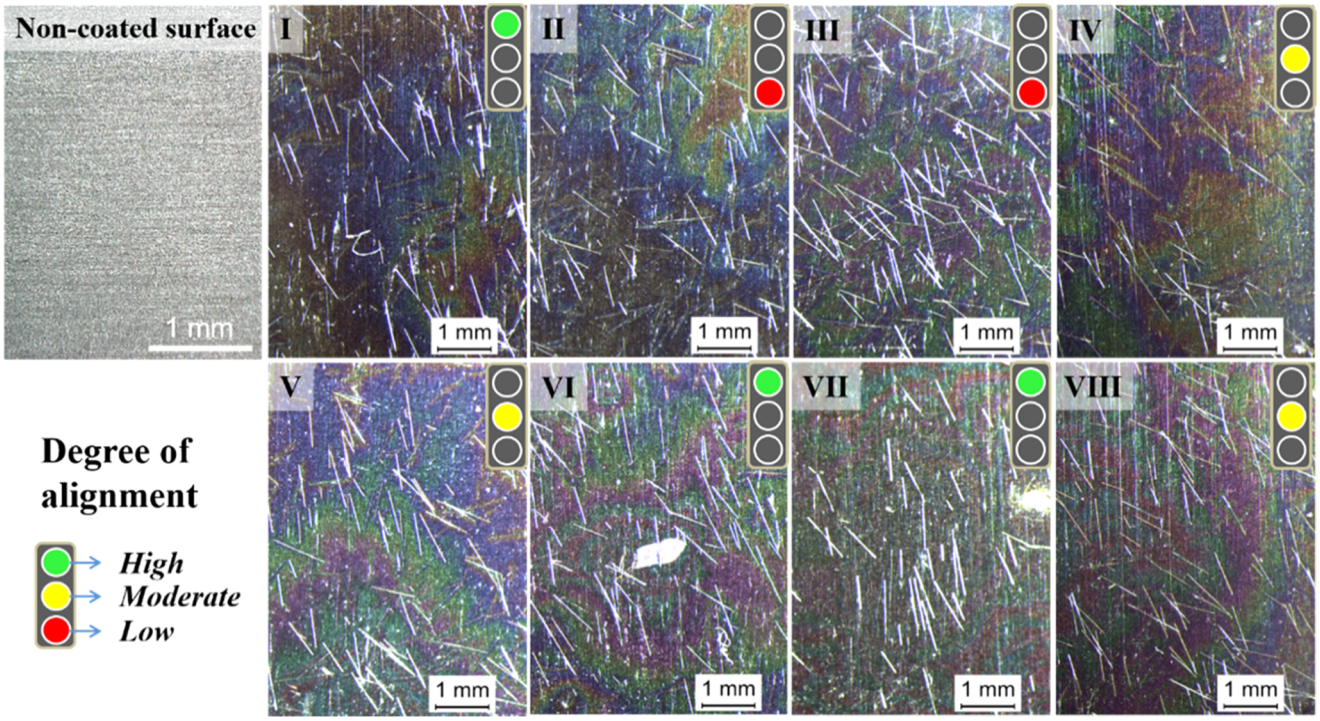

Figure 2. Alignment of sPGF in the deposited coatings ((I)−(VIII), compared to noncoated surface) prepared using different EPD parameters under horizontal electric field. The degree of alignment was assigned to three levels (high, moderate, and low levels) indicated by green, yellow, and red symbols, respectively.

OLYMPUS). After culture, the total RNA was extracted using TRIzol reagent (TaKARA Bio Inc, Shiga, Japan) and then converted into cDNA using PrimeScript RT Master Mix (TaKARA Bio Inc, Shiga, Japan) according to the manufacturer's instructions. The gene expression analysis was performed using CFX Manager System (CFX96TM, BioRad) and SYBR Premix Ex Taq II (TaKARA Bio Inc, Shiga, Japan) (n = 3). The relative transcript quantities of genes were normalized using GAPDH as the endogeneous reference gene. The primer sequences of the genes in this study are listed in Table 2 according to the literature.

2.4.4. Alkaline Phosphatase (ALP) Activity Test. The ALP activity of cells cultured with different concentrations of sPGF was tested using an ALP assay kit (Beyondtime Bio-Tech, China). It should be noted that osteogenic medium consisting of normal culture medium supplemented with 0.01 M β-glycerophosphate and 50 μg/mL vitamin C was used for this experiment. 1×10^5 cells per well were seeded with different concentrations of sPGF (0, 1, 5 mg/mL) and cultured for 7, 14, and 21 days. After culture, the samples were rinsed with PBS and lysed with 0.1% Triton X-100 solution for 30 min at 4 °C. Then, the solution was centrifuged at 3000 rpm for 2 min at 4 °C. 50 μL of the obtained supernatant was mixed with 50 μL chromogenic substrate and cultured for 30 min at 37 °C. The reaction was stopped by adding 100 μL terminal liquid. The ALP activity was measured in quadruplicate at 405 nm using a microplate reader.

2.5. Statistical Analysis. The results in this study were expressed as mean ± standard deviation (SD) from at least three independent experiments. The statistical analyses between the analyzed groups were carried out by SPSS 16.0 software based on the one-way analysis of variance. Statistical significance was considered when $P < 0.05$, 0.01, and 0.001.

3. RESULTS AND DISCUSSION

3.1. Orientation of sPGF with Vertical and Horizontal Electric Field. PAA is known as a biodegradable and biocompatible polymer, which is promising for the assembly of biomedical devices.[37,38] The role of PAA during the processing of sPGF−PAA composites can be assigned to three aspects. First, the high viscosity of PAA solution at pH 8 facilitated a stable dispersion of sPGF in the suspension. In addition, according to the findings on electrophoretic co-deposition of PAA−TiO_2 composite coatings,[39] it is assumed in the present experiment that sPGF were wrapped with PAA molecules leading to their negative surface charge and their further deposition on the positive electrode under the electric field. Third, the simultaneous deposition of PAA could act as the binder connecting sPGF to the surface of the substrate. As schematically shown in Figure 1, a vertical electric field was first designed to produce random orientation of sPGF in the sPGF−PAA coatings. Due to the effect of gravity and electrophoresis of PAA-charged sPGF, an accelerated sedimentation of sPGF could be achieved. On the other hand, horizontal electric field was applied with the aim to achieve one-dimensional orientation of sPGF in the deposited coating. During the withdrawal process of the coated electrode, the suspended as well as the weakly adhered sPGF were aligned on the PAA gel along the withdrawal direction, leading to a vertical orientation of sPGF in the coating.

Various suspension compositions and EPD parameters (Table 1) were used to achieve highly aligned sPGF in the deposited coating. The optical microscopic images of sPGF in the coating as well as the noncoated surfaces are shown in Figure 2. The degree of alignment was assigned to three levels, which are indicated by green, yellow, and red symbols, respectively. According to this visual inspection of the microscopic images, it was found that the deposition time played a negative effect on the degree of alignment as the amount of randomly deposited sPGF increased with the deposition time. The effect of deposition voltage on the degree of alignment was investigated when comparing the orientation of sPGF on samples I and II, which indicated a higher degree of sPGF orientation obtained at lower voltages. However,

DOI: 10.1021/acsami.8b01378
ACS Appl. Mater. Interfaces XXXX, XXX, XXX−XXX

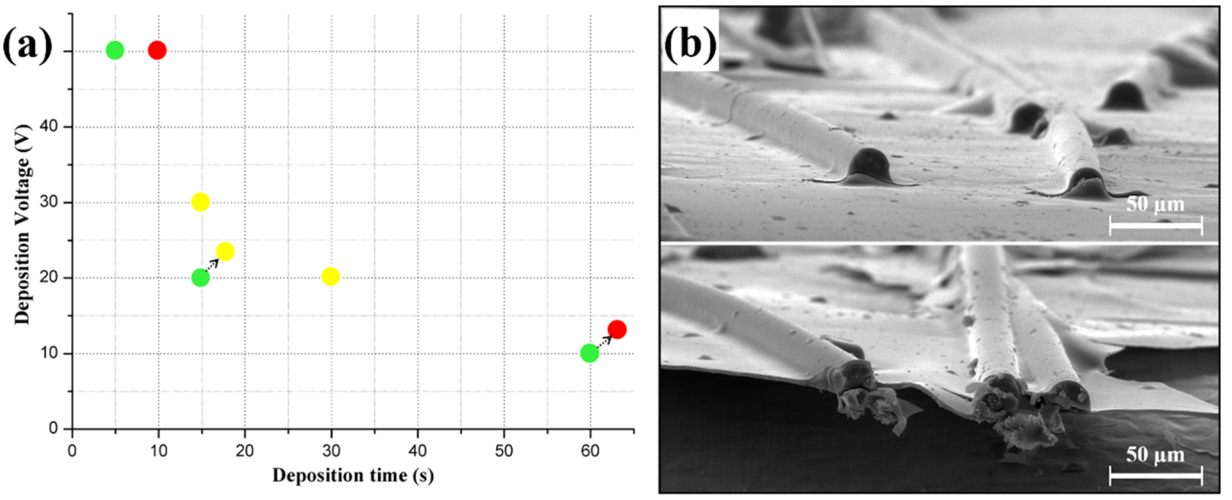

Figure 3. (a) Degree of sPGF alignment distributed in a deposition voltage vs deposition time plot. The arrows indicated the reduction of sPGF alignment with increasing sPGF concentration. (b) Cross-sectional SEM images of sample VI indicating that sPGF were partially embedded in the PAA layer.

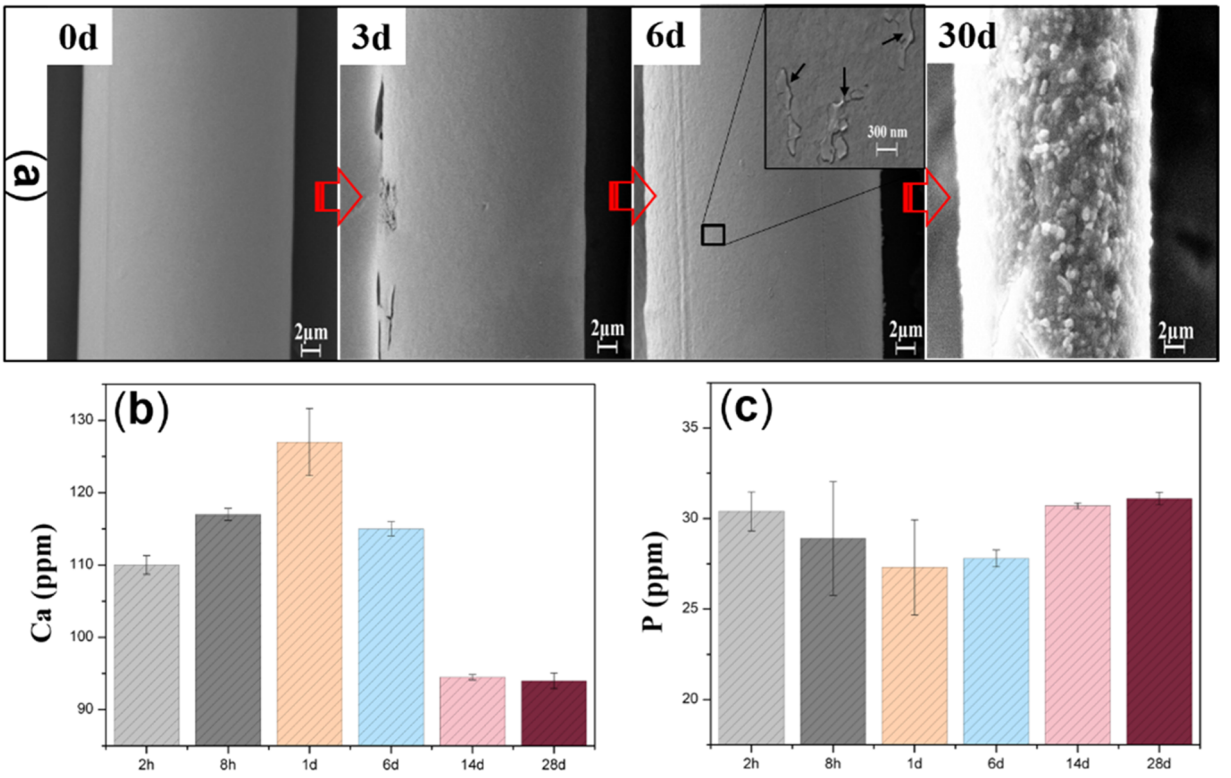

Figure 4. (a) Surface morphology of sPGF on the deposited sPGF–PAA coating as a function of incubation time in SBF. (b) Phosphorous and (c) calcium ion release profiles of sPGF in SBF (0.1 g/50 mL) for up to 28 days.

according to the observations on samples III–VI, it was found that the combination of high voltage with short deposition time is also beneficial for achieving a high degree of alignment. The effect of sPGF concentration on the degree of alignment was investigated by comparative studies from two groups (samples I vs III and samples VII vs VIII), which indicated a higher degree of sPGF orientation obtained using a lower concentration of sPGF.

The degree of sPGF alignment obtained using different EPD parameters and sPGF concentrations was plotted in a deposition voltage vs deposition time parameter window, as shown in Figure 3a. It can be concluded that both the sPGF–PAA concentration and the deposition voltage play an important role in the degree of orientation of sPGF. A high concentration of PAA (charger) or sPGF will significantly increase the deposit yield of randomly orientated sPGF on the coating. Similarly, a higher deposition voltage will lead to substantially higher driving force to accelerate the electrophoresis of sPGF in a short time. On the other hand, although the electrophoresis of sPGF will be probably restricted under a weak electric field, it is difficult to generate a relatively thick PAA gel with an extremely low voltage or short deposition time. In this way, if the deposition voltage is relatively low to trigger preferentially the electrophoresis of PAA molecules

DOI: 10.1021/acsami.8b01378
ACS Appl. Mater. Interfaces XXXX, XXX, XXX–XXX

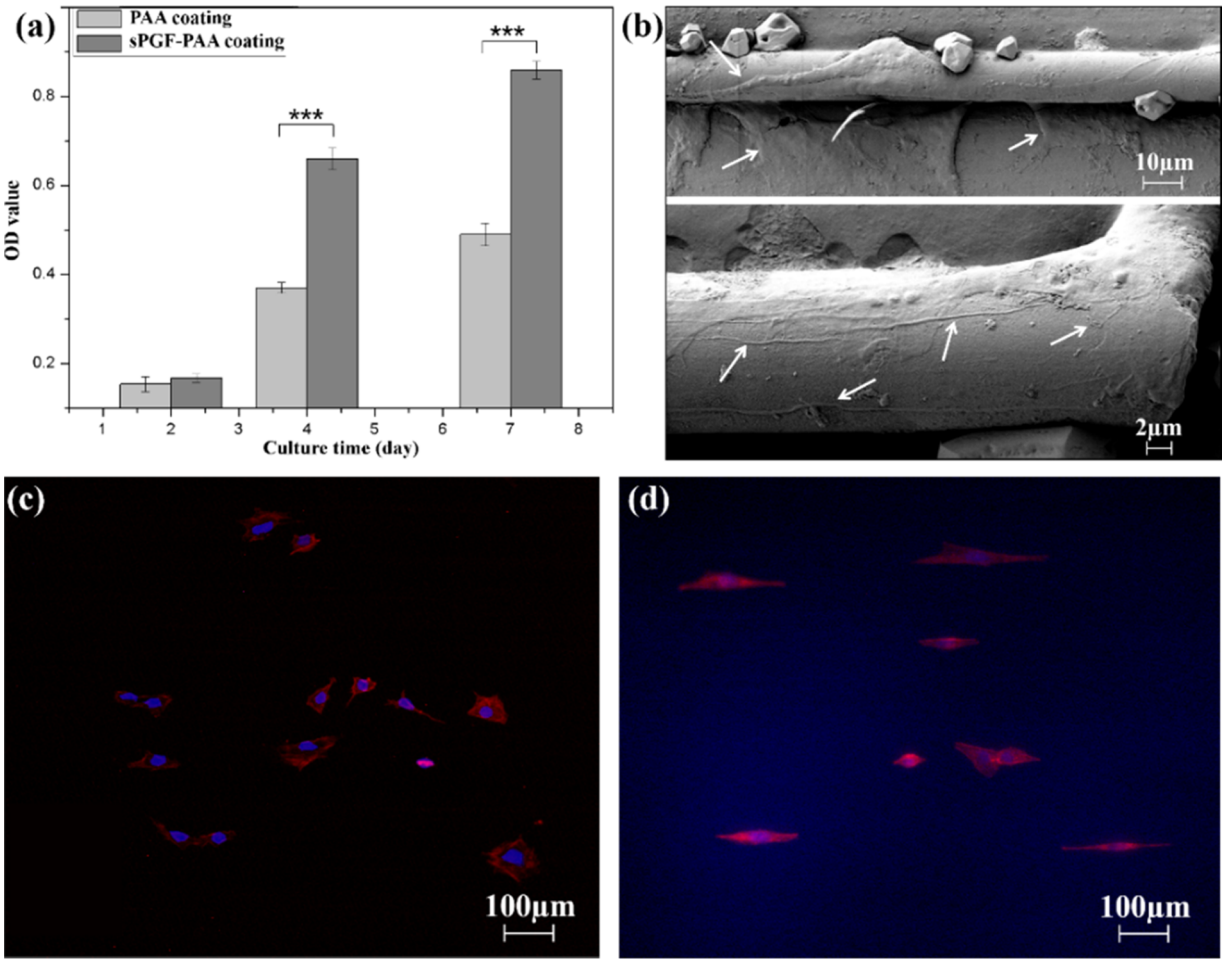

Figure 5. (a) Cell viability cultured on sPGF−PAA and PAA (control) coatings for 2, 4, and 7 days. (b) SEM images of the cells cultured on sPGF−PAA coatings for 2 days, and the arrows show the elongated skeleton and filaments along the fiber axis. Fluorescent images of stained cells on PAA (c) and sPGF−PAA (d) coatings for 2 days.

against the viscous suspension, a PAA-rich layer will be formed during EPD. For example, in sample I (deposition voltage and time of 10 V and 60 s, respectively), a relative thick PAA-rich layer was probably generated, resulting in a high degree of sPGF alignment during the withdrawal process (rearrangement of sPGF by fluid shear force). The PAA layer formed should be thick enough to support the adhesion of sPGF during the withdrawal process, e.g., the thickness of PAA layer on sample VI is only ∼3 μm according to the cross-sectional SEM image (Figure 3b), whereas sPGF were firmly adhered to the PAA matrix even after mechanical cutting. The enhancement of PAA deposition by increasing either deposition voltage or deposition time will simultaneously deteriorate the degree of sPGF alignment. Therefore, it is necessary to balance the deposition of PAA layer and the degree of sPGF alignment by using proper EPD parameters. In fact, there is a window rather than a point of PAA thickness to obtain oriented sPGF structures according to our experimental results. Based on this, there is another possibility to yield a PAA-rich layer is the use of high deposition voltage combined with short deposition time, as presented in sample VI (deposition voltage and time of 50 V and 5 s, respectively). Under such EPD conditions, sufficient amount of PAA gel can be generated, whereas few sPGF were able to adhere to the electrode during the short deposition period. Therefore, to ensure a high degree of alignment, a relatively thick PAA layer should be predeposited while minimizing the deposition of sPGF during EPD, which could be realized by applying a high voltage combined with a short time or a low voltage combined with a long time, as indicated by the green symbols in Figure 3.

3.2. In vitro Mineralization Study. The prepared sPGF−PAA coating was incubated in SBF for up to 30 days to evaluate their HA-forming ability as a marker of the coating bioactivity.[34] The surface morphology of sPGF as a function of incubation time is shown in Figure 4a. The retained sPGF on the coatings after SBF incubation also proves the high stability and robust adhesion strength of sPGF−PAA coatings. The as-deposited sPGF presented a smooth morphology and a uniform diameter of ∼20 μm. The surface of sPGF became rougher with longer incubation time, e.g., the fiber was completely wrapped with a rough layer after 7 days of incubation (shown in the inset for the day 7 sample). A slight reduction in fiber diameter was also observed (2−3 μm) after 30 days of incubation. Furthermore, the fiber was wrapped with a cauliflower-like layer of spherical nanoparticles, which could be assigned to the typical morphology of mineralized apatite crystals in SBF.[40,41]

Ion release profiles of raw sPGF incubated in SBF were analyzed to further elucidate the mineralization process of sPGF (sPGF/SBF ratio of 0.1 g/50 mL used in this experiment). The dynamic concentrations of calcium and phosphorous in the medium, which are closely associated with

DOI: 10.1021/acsami.8b01378
ACS Appl. Mater. Interfaces XXXX, XXX, XXX−XXX

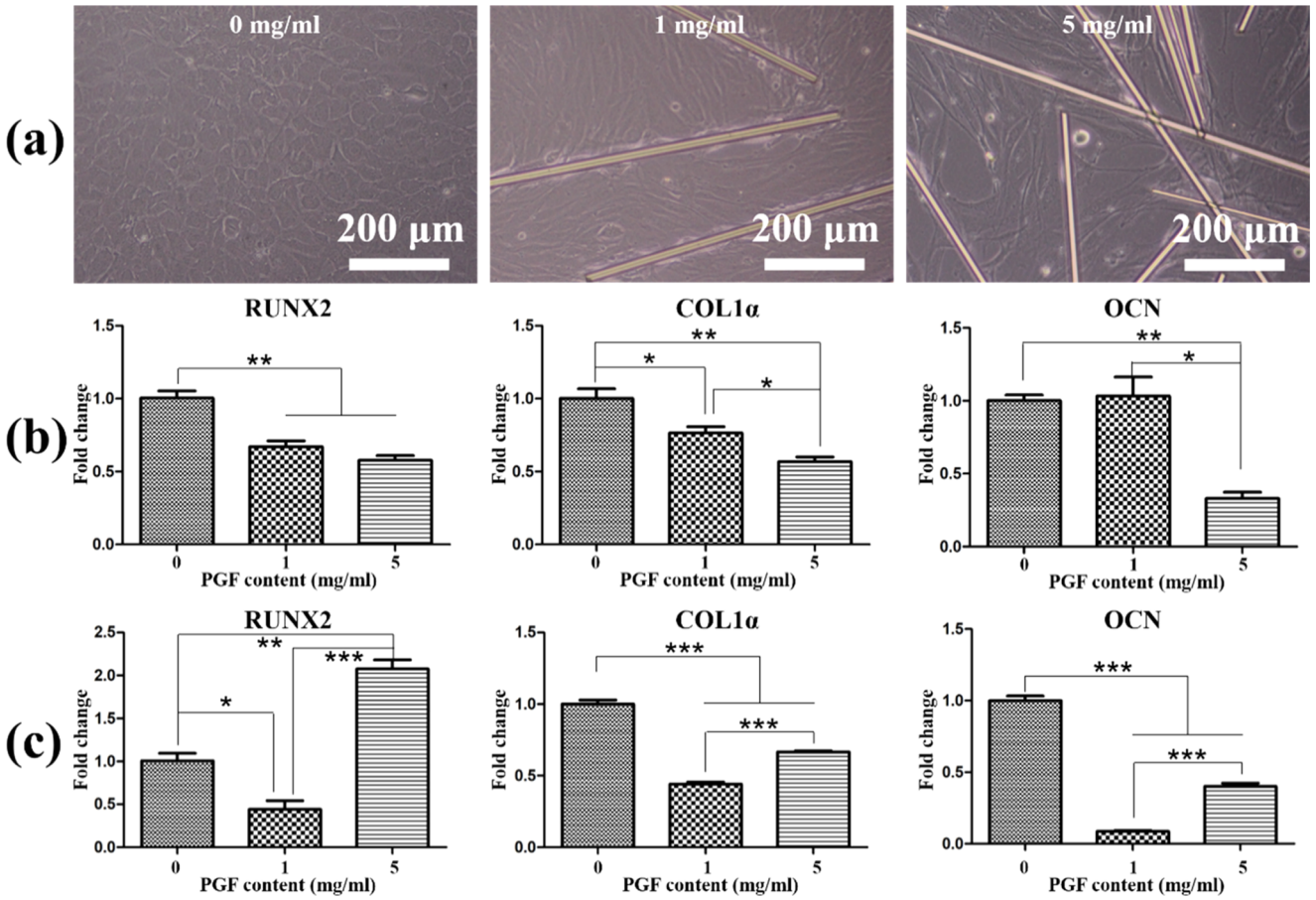

Figure 6. (a) Morphology of cells cultured with different concentrations of sPGF for 4 days. Osteogenesis-related gene expression of cells cultured with different concentrations of sPGF for (b) 7 days and (c) 14 days, respectively.

the formation of HA phase, are plotted in Figure 4b,c, respectively. According the SBF recipe provided by Kokubo et al.,[34] the initial concentrations of calcium and phosphorous in SBF are 2.5 (100) and 1 (31) mM (ppm), respectively. The ionic concentration of calcium and phosphorous should increase as a result of the continuous degradation of sPGF. However, the detected concentration of phosphorous exhibited an appreciable reduction during the first 6 days of incubation, whereas calcium exhibited a peak concentration of ~127 ppm after 1 day of incubation and then decreased to ~95 ppm after 14 days of incubation. It is reported that the degradation products of sPGF, including Ca^{2+} and PO_4^{3-} ions, will lead to the supersaturation in the surrounding SBF to accelerate apatite formation on the surface of the material.[40] According to the analyses of both the morphology and ion release profiles of sPGF in SBF, it could be concluded that the formation of a phosphate-rich layer was achieved at the early stage of SBF incubation. In addition, the constant ionic concentration after 14 days of incubation could be attributed to the equilibrium of reactions involving the degradation of sPGF and formation of apatite layers.

3.3. Cell Proliferation and Morphology on sPGF−PAA Coatings. Cell viability on both PAA and sPGF−PAA coatings was quantitatively studied by means of CCK-8 assay, as shown in Figure 5a. Both samples exhibited comparable cell viability after culture for 2 days, whereas a significantly higher cell viability ($P < 0.001$) on the sPGF−PAA coatings was detected after culture for 4 and 7 days. Both low- and high-magnification SEM images of cell morphology on day 2 samples are shown in Figure 5b. The cells tended to migrate to sPGF and spread along the fiber axis, e.g., the length of a cell spreading on the fiber is as high as 140 μm. In addition, it was observed that the cells tightly adhered on the fiber surface and produced an extremely elongated filopodia along the fiber axis. The obtained results suggested that the presence of sPGF could promote osteoblast proliferation. The bioactive composition of sPGF provides favorable surfaces to induce cell attachment. Moreover, the high aspect ratio of sPGF provides spaces for cell migration and proliferation. The cell morphology on PAA and sPGF−PAA coatings in a relatively large area was also observed, as shown in Figure 5c,d, respectively. The cells on the PAA coatings presented a tabular morphology, whereas those on the sPGF−PAA coatings presented an extremely elongated morphology under the same incubation conditions. The obtained results indicate that the sPGF will not only enhance cell proliferation but also regulate cell migration and morphology in vitro, e.g., accelerated oriented cell proliferation in one dimension was obtained by culturing cells on the sPGF−PAA coatings.

3.4. Osteogenic Differentiation Effect of sPGF. It is likely that both the composition and fiber orientation of the sPGF−PAA coating will influence the osteogenic activities. To understand the specific effect of sPGF on osteogenic differentiation while eliminating the possible interference induced by fiber alignment, sPGF (0, 1, and 5 mg/mL) were homogeneously dispersed in the culture medium with MC3T3-E1 cells

DOI: 10.1021/acsami.8b01378
ACS Appl. Mater. Interfaces XXXX, XXX, XXX−XXX

for a certain period. The selected concentrations of free sPGF were determined based on the deposit yield of sPGF in the coating (about 0.33−3.3 mg/cm^2). The morphology of cells cultured with different concentrations of sPGF for 4 days is shown in Figure 6a. The cells cultured without sPGF achieved complete confluence, whereas unconfluent areas increased with increasing sPGF concentration. Moreover, compared to the tabular geometry of the cells on the control sample, it was observed that the cells cultured with sPGF exhibited an elongated geometry along the fiber axis or between the fibers, which is probably caused by stretching of the cell filopodia during migration to sPGF and during proliferation along the sPGF axes. The expression of osteogenesis-related genes of MC3T3-E1 cell, including RUNX2, COL1α, and OCN, cultured with different concentrations of sPGF for 7 and 14 days is shown in Figure 6b,c, respectively. At day 7, the expression levels of all genes on sPGF-containing samples were slightly lower than those on the control group (except OCN expression with 1 mg/mL of sPGF), and the gene expression became lower with increasing sPGF concentration. At day 14, the relative gene expression was significantly increased with increasing sPGF concentration; however, only the RUNX2 with 10 mg/mL of sPGF exhibited a higher expression level compared to the control group.

The ALP activity is considered a phenotypic marker for the mature osteoblast, which is expected to be upregulated during the early differentiation period, and gradually downregulated at the later differentiation period.[42,43] The ALP activity of cells cultured with different concentrations of PGF for 7, 14, and 21 days is comparatively shown in Figure 7. After 7 days, the ALP

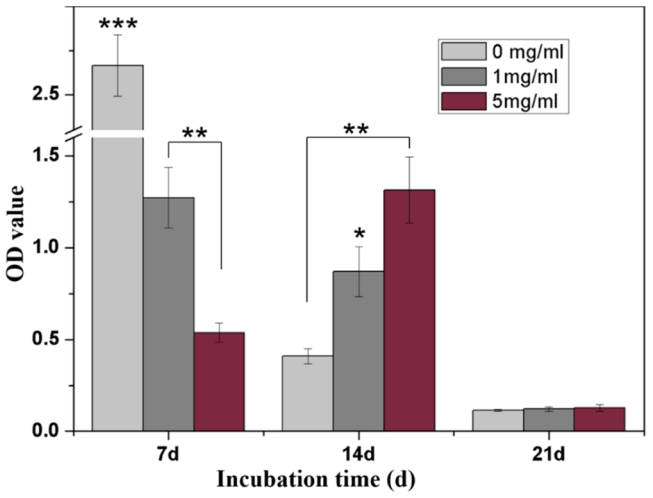

Figure 7. ALP activity of cells cultured with different concentrations of PGF. Error bars represent means ± SD for $n = 4$ (*$P < 0.05$, **$P < 0.01$, ***$P < 0.001$).

activity was significantly minimized with increasing sPGF concentration. Moreover, the ALP activity was further reduced on the sPGF-free sample and the sample with 1 mg/mL of sPGF after culture for 14 days, whereas the sample with 5 mg/mL of sPGF exhibited increased and higher ALP activity than the other two samples. After culture for 21 days, all samples exhibited a substantially lowered ALP activity and no significant difference was found according to the statistical analysis.

According to the previous CCK-8 analysis, significantly enhanced cell proliferation was detected when culturing with sPGF. Meanwhile, the increase in the unconfluent area in Figure 6a, probably due to preferential cell attachment on the sPGF surfaces, indicated that a prolonged period of cell proliferation is needed to cover the entire surface area. The obtained results suggest that the delayed osteogenic differentiation with increasing sPGF concentration at day 7 may be attributed to the preferential cell proliferation against cell differentiation.[44,45] In addition, the surface topography of a material also plays an important role in the osteogenic functions by regulating the morphological characteristics of the cell body and nucleus.[46] It was reported that elongated human mesenchymal stem cells (hMSCs), induced by microgrooved surfaces (2.75 μm), exhibited lowered osteogenesis compared to polygonal-like hMSCs cultured on flat surfaces, which is positively correlated with the downexpression of several cell morphological indexes, including integrin β1 and N-cadherin.[47] Considering that sPGF used in this study possessed a diameter comparable to the size of the reported microgrooves, it is considered that the elongation of MC3T3-E1 cells induced by sPGF, with respect to the tabular morphology of cells in the control group, should be another important reason for their downexpression of osteogenic genes at day 7. After culture for 14 days, the significant upexpression of osteogenic marker genes with increasing sPGF concentration can be ascribed to different reasons. On the one hand, the depletion of unconfluent space may induce the transition from cell proliferation to cell differentiation stage, and the higher cell density with increasing sPGF concentration should contribute to an increased gene expression level. On the other hand, the formation of a phosphate-rich layer became increasingly obvious at longer incubation times (Figure 4), and such a favorable surface chemistry should lead to a positive influence on the seen osteogenic activity. The long-term ALP activity analysis also confirmed the delayed osteogenic activity with an increasing sPGF concentration at day 7. The further decreased ALP activity of the control group was in accordance with the expression trend during osteogenic differentiation.[43] However, the higher ALP activity on PGF-containing samples at day 14, compared to the control group, indicated that the presence of sPGF positively affects the osteogenesis at the later incubation period. According to our findings from cell culture experiments, significantly enhanced and directional cell proliferation was obtained in the presence of sPGF, which is of great interest for bone defect repair. Moreover, delayed but significantly enhanced osteogenic differentiation was observed with the increase in sPGF concentration. The long-term mineralization of sPGF as well as the in vivo performance of the coatings will be considered in future studies to assess the true potential of the coatings in orthopedic applications. We expect that the bioactive characteristic of sPGF will further facilitate osteogenic activity at different periods of bone regeneration.

4. CONCLUSIONS

sPGF−PAA composite coatings with random and one-dimensional orientation of sPGF were successfully fabricated on stainless steel plates according to vertical and horizontal EPD, respectively. A vertical electric field configuration can effectively yield a sPGF−PAA composite coating with random orientation of sPGF. By applying a horizontal electric field, a PAA gel layer was first electrodeposited in situ on the anode, followed by the fluid shear force-induced alignment of sPGF along the withdrawal direction of the deposition electrode. Both the EPD parameters and the sPGF concentration play important roles in determining the degree of alignment during horizontal

DOI: 10.1021/acsami.8b01378
ACS Appl. Mater. Interfaces XXXX, XXX, XXX−XXX

EPD. The prerequisite for achieving highly aligned sPGF structures is the formation of a PAA-rich layer using a high deposition and/or a short deposition time, which could then assist the adhesion and arrangement of sPGF during the withdrawal process. Continuous mineralization, characterized by the formation of a phosphate-rich layer around sPGF was achieved during incubation in SBF. In addition, the presence of highly aligned sPGF in the composite coating not only enhanced osteoblastic proliferation but also regulated cell migration and spreading in one-dimensional orientation. Although delayed osteogenic differentiation with increasing sPGF concentration was detected in the initial stage, it is expected that bioactive sPGF coatings with controllable orientation are promising for directional bone defect repair. The versatility of EPD technique to manipulate macroscopic glass fibers to obtain oriented coatings was validated in this study. Ongoing investigations have proven that similar fiber structures could be obtained using different composition of sPGF and even polymer fibers, and further investigations will consider the effect of the oriented sPGF−PAA coatings on bone bonding in vivo.

AUTHOR INFORMATION

Corresponding Authors

*E-mail: lutinglixinxin@nwpu.edu.cn (T.L.L.).

*E-mail: aldo.boccaccini@ww.uni-erlangen.de (A.R.B.).

ORCID

Qiang Chen: 0000-0001-8829-0679

Xianhu Liu: 0000-0002-4975-3586

Aldo R. Boccaccini: 0000-0002-7377-2955

Notes

The authors declare no competing financial interest.

ACKNOWLEDGMENTS

We thank Dr. Xiao Lin (Key Laboratory for Space Bioscience and Biotechnology, School of Life Sciences, Northwestern Polytechnical University) for experimental support. Financial supports for this work from the State Key Laboratory of Solidification Processing in NWPU (SKLSP201715) and the Fundamental Research Funds for the Central Universities (No. G2016KY0103) are acknowledged.

REFERENCES

(1) Ince, A.; Rupp, J.; Frommelt, L.; Katzer, A.; Gille, J.; Lohr, J. F. Is "Aseptic" Loosening of the Prosthetic Cup After Total Hip Replacement Due to Nonculturable Bacterial Pathogens in Patients with Low-Grade Infection? *Clin. Infect. Dis.* **2004**, *39*, 1599−1603.

(2) Chen, Q. Z.; Thouas, G. A. Metallic Implant Biomaterials. *Mater. Sci. Eng., R* **2015**, *87*, 1−57.

(3) Hammond, P. T. Building Biomedical Materials Layer-by-Layer. *Mater. Today* **2012**, *15*, 196−206.

(4) Goodman, S. B.; Yao, Z. Y.; Keeney, M.; Yang, F. The Future of Biologic Coatings for Orthopaedic Implants. *Biomaterials* **2013**, *34*, 3174−3183.

(5) Song, J.; Chen, Q.; Zhang, Y.; Diba, M.; Kolwijck, E.; Shao, J. L.; Jansen, J. A.; Yang, F.; Boccaccini, A. R.; Leeuwenburgh, S. C. G. Electrophoretic Deposition of Chitosan Coatings Modified with Gelatin Nanospheres to Tune the Release of Antibiotics. *ACS Appl. Mater. Interfaces* **2016**, *8*, 13785−13792.

(6) Riool, M.; de Breij, A.; de Boer, L.; Kwakman, P. H. S.; Cordfunke, R. A.; Cohen, O.; Malanovic, N.; Emanuel, N.; Lohner, K.; Drijfhout, J. W.; Nibbering, P. H.; Zaat, S. A. J. Controlled Release of LL-37-Derived Synthetic Antimicrobial and Anti-Biofilm Peptides SAAP-145 and SAAP-276 Prevents Experimental Biomaterial-Associated *Staphylococcus aureus* Infection. *Adv. Funct. Mater.* **2017**, *27*, No. 1606623.

(7) Hench, L. L. Bioceramics - from Concept to Clinic. *J. Am. Ceram. Soc.* **1991**, *74*, 1487−1510.

(8) Geuli, O.; Metoki, N.; Eliaz, N.; Mandler, D. Electrochemically Driven Hydroxyapatite Nanoparticles Coating of Medical Implants. *Adv. Funct. Mater.* **2016**, *26*, 8003−8010.

(9) Chen, Q.; Garcia, R. P.; Munoz, J.; de Larraya, U. P.; Garmendia, N.; Yao, Q. Q.; Boccaccini, A. R. Cellulose Nanocrystals-Bioactive Glass Hybrid Coating as Bone Substitutes by Electrophoretic Co-deposition: In Situ Control of Mineralization of Bioactive Glass and Enhancement of Osteoblastic Performance. *ACS Appl. Mater. Interfaces* **2015**, *7*, 24715−24725.

(10) Pishbin, F.; Mourino, V.; Flor, S.; Kreppel, S.; Salih, V.; Ryan, M. P.; Boccaccini, A. R. Electrophoretic Deposition of Gentamicin-Loaded Bioactive Glass/Chitosan Composite Coatings for Orthopaedic Implants. *ACS Appl. Mater. Interfaces* **2014**, *6*, 8796−8806.

(11) Sharmin, N.; Rudd, C. D. Structure, Thermal Properties, Dissolution Behaviour and Biomedical Applications of Phosphate Glasses and Fibres: A Review. *J. Mater. Sci.* **2017**, *52*, 8733−8760.

(12) Ahmed, I.; Collins, C. A.; Lewis, M. P.; Olsen, I.; Knowles, J. C. Processing, Characterisation and Biocompatibility of Iron-Phosphate Glass Fibres for Tissue Engineering. *Biomaterials* **2004**, *25*, 3223−3232.

(13) Vitale-Brovarone, C.; Novajra, G.; Lousteau, J.; Milanese, D.; Raimondo, S.; Fornaro, M. Phosphate Glass Fibres and Their Role in Neuronal Polarization and Axonal Growth Direction. *Acta Biomater.* **2012**, *8*, 1125−1136.

(14) Joo, N. Y.; Knowles, J. C.; Lee, G. S.; Kim, J. W.; Kim, H. W.; Son, Y. J.; Hyun, J. K. Effects of Phosphate Glass Fiber-Collagen Scaffolds on Functional Recovery of Completely Transected Rat Spinal Cords. *Acta Biomater.* **2012**, *8*, 1802−1812.

(15) Kim, Y. P.; Lee, G. S.; Kim, J. W.; Kim, M. S.; Ahn, H. S.; Lim, J. Y.; Kim, H. W.; Son, Y. J.; Knowles, J. C.; Hyun, J. K. Phosphate Glass Fibres Promote Neurite Outgrowth and Early Regeneration in a Peripheral Nerve Injury Model. *J. Tissue Eng. Regener. Med.* **2015**, *9*, 236−246.

(16) Jiang, X.; Cao, H. Q.; Shi, L. Y.; Ng, S. Y.; Stanton, L. W.; Chew, S. Y. Nanofiber Topography and Sustained Biochemical Signaling Enhance Human Mesenchymal Stem Cell Neural Commitment. *Acta Biomater.* **2012**, *8*, 1290−1302.

(17) Li, Y.; Dai, X.; Bai, Y.; Liu, Y.; Wang, Y.; Liu, O.; Yan, F.; Tang, Z.; Zhang, X.; Deng, X. Electroactive BaTiO3 Nanoparticle-Functionalized Fibrous Scaffolds Enhance Osteogenic Differentiation of Mesenchymal Stem Cells. *Int. J. Nanomed.* **2017**, *12*, 4007−4018.

(18) Reinwald, Y.; El Haj, A. J. Hydrostatic Pressure in Combination with Topographical Cues Affects the Fate of Bone Marrow-Derived Human Mesenchymal Stem Cells for Bone Tissue Regeneration. *J. Biomed. Mater. Res., Part A* **2018**, *106*, 629−640.

(19) Rowland, D. C.; Aquilina, T.; Klein, A.; Hakimi, O.; Alexis-Mouthuy, P.; Carr, A. J.; Snelling, S. J. A Comparative Evaluation of the Effect of Polymer Chemistry and Fiber Orientation on Mesenchymal Stem Cell Differentiation. *J. Biomed. Mater. Res., Part A* **2016**, *104*, 2843−2853.

(20) Gao, X.; Song, J.; Zhang, Y.; Xu, X.; Zhang, S.; Ji, P.; Wei, S. Bioinspired Design of Polycaprolactone Composite Nanofibers as Artificial Bone Extracellular Matrix for Bone Regeneration Application. *ACS Appl. Mater. Interfaces* **2016**, *8*, 27594−27610.

(21) Valente, T. A. M.; Silva, D. M.; Gomes, P. S.; Fernandes, M. H.; Santos, J. D.; Sencadas, V. Effect of Sterilization Methods on Electrospun Poly(lactic acid) (PLA) Fiber Alignment for Biomedical Applications. *ACS Appl. Mater. Interfaces* **2016**, *8*, 3241−3249.

(22) Ma, J.; He, X. Z.; Jabbari, E. Osteogenic Differentiation of Marrow Stromal Cells on Random and Aligned Electrospun Poly(L-lactide) Nanofibers. *Ann. Biomed. Eng.* **2011**, *39*, 14−25.

(23) Kantawong, F.; Burgess, K. E. V.; Jayawardena, K.; Hart, A.; Burchmore, R. J.; Gadegaard, N.; Oreffo, R. O. C.; Dalby, M. J. Whole Proteome Analysis of Osteoprogenitor Differentiation Induced by

DOI: 10.1021/acsami.8b01378
ACS Appl. Mater. Interfaces XXXX, XXX, XXX−XXX

Disordered Nanotopography and Mediated by ERK Signalling. *Biomaterials* **2009**, *30*, 4723−4731.
(24) Wang, W.; Liu, Q.; Zhang, Y. M.; Zhao, L. Z. Involvement of ILK/ERK1/2 and ILK/p38 Pathways in Mediating the Enhanced Osteoblast Differentiation by Micro/Nanotopography. *Acta Biomater.* **2014**, *10*, 3705−3715.
(25) Zhao, C.; Xia, L. G.; Zhai, D.; Zhang, N.; Liu, J. Q.; Fang, B.; Chang, J.; Lin, K. L. Designing Ordered Micropatterned Hydroxyapatite Bioceramics to Promote the Growth and Osteogenic Differentiation of Bone Marrow Stromal Cells. *J. Mater. Chem. B* **2015**, *3*, 968−976.
(26) Aminuddin, N. I.; Ahmad, R.; Akbar, S. A.; Pingguan-Murphy, B. Osteoblast and Stem Cell Response to Nanoscale Topographies: A Review. *Sci. Technol. Adv. Mater.* **2016**, *17*, 698−714.
(27) Abou Neel, E. A.; Pickup, D. M.; Valappil, S. P.; Newport, R. J.; Knowles, J. C. Bioactive functional materials: a perspective on phosphate-based glasses. *J. Mater. Chem.* **2009**, *19*, 690−701.
(28) Boccaccini, A. R.; Keim, S.; Ma, R.; Li, Y.; Zhitomirsky, I. Electrophoretic Deposition of Biomaterials. *J. R. Soc., Interface* **2010**, *7*, S581−S613.
(29) Yao, Q.; Jing, J. J.; Zeng, Q. Y.; Lu, T. L.; Liu, Y.; Zheng, X.; Chen, Q. Bilayered BMP2 Eluting Coatings on Graphene Foam by Electrophoretic Deposition: Electroresponsive BMP2 Release and Enhancement of Osteogenic Differentiation. *ACS Appl. Mater. Interfaces* **2017**, *9*, 39962−39970.
(30) Chen, Q.; de Larraya, U. P.; Garmendia, N.; Lasheras-Zubiate, M.; Cordero-Arias, L.; Virtanen, S.; Soccaccini, A. R. Electrophoretic Deposition of Cellulose Nanocrystals (CNs) and CNs/Alginate Nanocomposite Coatings and Free Standing Membranes. *Colloids Surf., B* **2014**, *118*, 41−48.
(31) Felfel, R. M.; Ahmed, I.; Parsons, A. J.; Walker, G. S.; Rudd, C. D. In Vitro Degradation, Flexural, Compressive and Shear Properties of Fully Bioresorbable Composite Rods. *J. Mech. Behav. Biomed. Mater.* **2011**, *4*, 1462−1472.
(32) Kato, N.; Schuetz, P.; Fery, A.; Caruso, F. Thin Multilayer Films of Weak Polyelectrolytes on Colloid Particles. *Macromolecules* **2002**, *35*, 9780−9787.
(33) Wang, Y.; Deen, I.; Zhitomirsky, I. Electrophoretic Deposition of Polyacrylic Acid and Composite Films Containing Nanotubes and Oxide Particles. *J. Colloid Interface Sci.* **2011**, *362*, 367−374.
(34) Kokubo, T.; Takadama, H. How Useful is SBF in Predicting in Vivo Bone Bioactivity? *Biomaterials* **2006**, *27*, 2907−2915.
(35) Cerruti, M.; Greenspan, D.; Powers, K. Effect of pH and Ionic Strength on the Reactivity of Bioglass((R)) 45S5. *Biomaterials* **2005**, *26*, 1665−1674.
(36) Hu, L.-f.; Li, J.-B.; Qian, A. R.; Wang, F.; Shang, P. Mineralization Initiation of MC3T3-E1 Preosteoblast is Suppressed Under Simulated Microgravity Condition. *Cell Biol. Int.* **2015**, *39*, 364−372.
(37) Stuart, M. A. C.; Huck, W. T. S.; Genzer, J.; Muller, M.; Ober, C.; Stamm, M.; Sukhorukov, G. B.; Szleifer, I.; Tsukruk, V. V.; Urban, M.; Winnik, F.; Zauscher, S.; Luzinov, I.; Minko, S. Emerging Applications of Stimuli-Responsive Polymer Materials. *Nat. Mater.* **2010**, *9*, 101−113.
(38) Xiong, L.; Yang, T. S.; Yang, Y.; Xu, C. J.; Li, F. Y. Long-Term in Vivo Biodistribution Imaging and Toxicity of Polyacrylic Acid-Coated Upconversion Nanophosphors. *Biomaterials* **2010**, *31*, 7078−7085.
(39) Yoshioka, T.; Chavez-Valdez, A.; Roether, J. A.; Schubert, D. W.; Boccaccini, A. R. AC Electrophoretic Deposition of Organic-Inorganic Composite Coatings. *J. Colloid Interface Sci.* **2013**, *392*, 167−171.
(40) Massera, J.; Ahmed, I.; Petit, L.; Aallos, V.; Hupa, L. Phosphate-Based Glass Fiber vs. Bulk Glass: Change in Fiber Optical Response to Probe in Vitro Glass Reactivity. *Mater. Sci. Eng., C* **2014**, *37*, 251−257.
(41) Zheng, K.; Wu, Z. Y.; Wei, J.; Russel, C.; Liang, W.; Boccaccini, A. R. Preparation and Characterization of Fibrous Chitosan-Glued Phosphate Glass Fiber Scaffolds for Bone Regeneration. *J. Mater. Sci.: Mater. Med.* **2015**, *26*, 224.
(42) Chen, Q.; Li, W.; Yao, Q. Q.; Liang, R. F.; Perez-Garcia, R.; Munoz, J.; Boccaccini, A. R. Multilayered Drug Delivery Coatings Composed of Daidzein-Loaded PHBV Microspheres Embedded in a Biodegradable Polymer Matrix by Electrophoretic Deposition. *J. Mater. Chem. B* **2016**, *4*, 5035−5045.
(43) Frith, J.; Genever, P. Transcriptional Control of Mesenchymal Stem Cell Differentiation. *Transfus. Med. Hemother.* **2008**, *35*, 216−227.
(44) Chang, B.; Song, W.; Han, T. X.; Yan, J.; Li, F. P.; Zhao, L. Z.; Kou, H. C.; Zhang, Y. M. Influence of Pore Size of Porous Titanium Fabricated by Vacuum Diffusion Bonding of Titanium Meshes on Cell Penetration and Bone Ingrowth. *Acta Biomater.* **2016**, *33*, 311−321.
(45) Yan, J.; Zhang, C. C.; Zhao, Y. T.; Cao, C.; Wu, K. M.; Zhao, L. Z.; Zhang, Y. M. Non-Viral Oligonucleotide AntimiR-138 Delivery to Mesenchymal Stem Cell Sheets and the Effect on Osteogenesis. *Biomaterials* **2014**, *35*, 7734−7749.
(46) Gong, T.; Xie, J.; Liao, J. F.; Zhang, T.; Lin, S. Y.; Lin, Y. F. Nanomaterials and Bone Regeneration. *Bone Res.* **2015**, *3*, No. 15029.
(47) Kim, J.; Kim, H. N.; Lim, K. T.; Kim, Y.; Seonwoo, H.; Park, S. H.; Lim, H. J.; Kim, D. H.; Suh, K. Y.; Choung, P. H.; Choung, Y. H.; Chung, J. H. Designing Nanotopographical Density of Extracellular Matrix for Controlled Morphology and Function of Human Mesenchymal Stem Cells. *Sci. Rep.* **2013**, *3*, No. 3552.

DOI: 10.1021/acsami.8b01378
ACS Appl. Mater. Interfaces XXXX, XXX, XXX−XXX